APS physics

CHORUS

This is the accepted manuscript made available via CHORUS. The article has been published as:

# Long-lived nonequilibrium states in the Hubbard model with an electric field

Alexander V. Joura, J. K. Freericks, and Alexander I. Lichtenstein

Phys. Rev. B **91**, 245153 — Published 26 June 2015

DOI: 10.1103/PhysRevB.91.245153

# Long-lived nonequilibrium states in the Hubbard model with an electric field

Alexander V. Joura,[1,2,*] J. K. Freericks,[3] and Alexander I. Lichtenstein[1,2,†]

[1]*Institute of Theoretical Physics, University of Hamburg, Jungiusstrasse 9, D-20355 Hamburg, Germany*
[2]*European XFEL GmbH, Albert-Einstein-Ring 19, D-22671 Hamburg, Germany*
[3]*Department of Physics, Georgetown University, Washington, DC 20057-0995, USA*

(Dated: April 15, 2015)

We study the single-band Hubbard model in the presence of a large spatially uniform electric field out of equilibrium. Using the Keldysh nonequilibrium formalism, we solve the problem using perturbation theory in the Coulomb interaction $U$. We present numerical results for the charge current, the total energy of the system and the double occupancy on an infinite-dimensional hypercubic lattice with nearest-neighbor hopping. The system is isolated from an external bath and is in the paramagnetic state. We show that an electric field pulse can drive the system to a steady nonequilibrium state, which does not evolve into a thermal state. We compare results obtained within second-order perturbation theory (SOPT), self-consistent SOPT and iterated perturbation theory (IPT). We also discuss the importance of initial conditions for a system which is not coupled to an external bath.

PACS numbers: 71.27.+a, 71.10.Fd, 72.20.Ht, 71.15.-m

## I. INTRODUCTION

The recent growth of experimental interest in systems driven out of equilibrium[1] has stimulated a lot of theoretical activity to explain these experiments. The observation of Bloch oscillations in ultracold atoms[2] and the corresponding theoretical treatment of the fermionic Hubbard model in an additional linear potential[3] give a new interesting twist to the classical problem of the electric current on a lattice and require nonequilibrium many-body methods, developed by Kadanoff and Baym[4], and Keldysh[5].

The nonequilibrium dynamical mean-field theory (NE-DMFT), introduced by Schmidt and Monien[6] and Freericks, *et al.*[7], is a combination of the equilibrium[8] and nonequilibrium DMFT formalisms. It has made feasible nonperturbative calculations of many-body models driven out of equilibrium by external fields. While for the Falicov-Kimball (FK) model it was possible to formulate a definitive numerically exact DMFT algorithm[7,9], for the Hubbard model, one currently has to choose between quantum Monte Carlo methods and perturbative calculations. The nonequilibrium continuous time quantum Monte Carlo (NE CT-QMC) technique[10,11] is a powerful calculational tool, but it suffers from the so-called phase problem, which renders its usage to relatively short real times. Hence, most Hubbard model results for NE-DMFT are perturbative.

Recently, there has been a significant interest in the many-body thermalization of isolated systems[12]. Cramer, *et al.*[13] studied the Bose-Hubbard model and provided general arguments that after the interaction quench to a noninteracting state the system will relax to a nonthermal state. The opposite case of an interaction quench to a nonzero interaction, was studied by Eckstein and Kollar[14] for the Falicov-Kimball model on the Bethe lattice using a numerically exact NE-DMFT approach. It was found that the system never thermalizes. The inability of the system to thermalize was attributed to the presence of an infinite number of conserved quantities for the Falicov-Kimball model, due to the presence of immobile $f$-particles. Later Eckstein, *et al.*[15] found that the Hubbard model directly thermalizes only for interactions close to $U_c^{dyn}$. For quenches to interactions both smaller and larger, the system is initially trapped in a quasistationary nonthermal state, called a prethermalized state. Using the quantum Bolzmann equation, Moeckel and Kehrein[16] argued that for small values of the Coulomb interaction these prethermalized states eventually evolve into thermal states on timescales of the order of $\tau_{therm} \sim \rho_0^{-3}(0)U^{-4}$. However, there is evidence[17] that the existence of the prethermalized state is an artifact of the infinite dimensional limit.

Despite the fact that the prethermalized states cannot be described by a simple Fermi distribution, interaction quenches in the Hubbard model usually do lead to distributions qualitatively similar to Fermi ones. In particular the double occupancy in prethermalized states decreases as the repulsive interaction increases. An interesting change in behavior happens when, instead of quenching the interaction, one quenches an external electric field. When a DC field is applied to a system, it is predicted to heat up[18] to $T = \infty$ as the current goes to zero, thus providing an example of thermalization. Fotso, *et al.*[19], predict that this is just one of five different scenarios that can occur for such a field quench. Tsuji, *et al.*[20] studied the Hubbard model under the application of an electric pulse to the system, which is initially prepared in an interacting thermal state (no $U$-quench). They found that by tuning the pulse parameters it is possible to achieve a long-lived state, corresponding to a thermal state with a negative temperature, where electrons behave as though they attract to each other.

In this article, we study the behaviour of the Hubbard model in the presence of a uniform electric field. In particular, we show how a combination of the interaction

quench and an electric field pulse can drive the system to a long-lived nonequilibrium state, where the particle distribution does not resemble a Fermi distribution. These results show the possibility of prethermalization-like behavior even for systems where double occupancies can easily form, which is a counterpart to strongly coupled systems, which have been argued to have prethermalized states because it becomes difficult to release the energy of a double occupancy when the interaction is large. Our approximate calculations show that the system conserves its exotic properties even for times comparable to theoretical estimates of the lifetime of prethermalized states. In Sec. II, we develop the formalism, in Sec. III, we show the numerical results, and in Sec. IV, we present our conclusions.

## II. FORMALISM

We consider the single-band Hubbard model on a $d$-dimensional Bravais lattice with the Hamiltonian

$$\hat{H}(t) = \sum_{ij,\sigma} T_{ij}(t)\hat{c}^\dagger_{i\sigma}\hat{c}_{j\sigma} - \mu_0 \sum_{i\sigma} \hat{c}^\dagger_{i\sigma}\hat{c}_{i\sigma} + U(t)\sum_i \hat{n}_{i\uparrow}\hat{n}_{i\downarrow} \tag{1}$$

where $T_{ij}(t)$ are hopping coefficients with the time-dependence described below, $\mu_0$ is the noninteracting chemical potential and $U(t)$ is the on-site Coulomb interaction (which can also be time-dependent). We describe the external spatially uniform electric field via the vector potential $\mathbf{A}(t)$

$$\mathbf{E}(t) = -\partial_t \mathbf{A}(t)\ . \tag{2}$$

The Peierls substitution[21] is used to account for the electric field in the Hamiltonian, so the hopping matrix elements satisfy

$$T_{ij}(t) = T_{ij}\exp[-i\mathbf{A}(t)\cdot(\mathbf{R}_j - \mathbf{R}_i)]\ . \tag{3}$$

In $\mathbf{k}$-space, the noninteracting part of the Hamiltonian in Eqs. (1) and (3) becomes diagonal

$$\hat{H}_0(t) = \sum_{\mathbf{k}} \xi(\mathbf{k}-\mathbf{A}(t))\hat{c}^\dagger_{\mathbf{k}\sigma}\hat{c}_{\mathbf{k}\sigma} \tag{4}$$

where $\xi(\mathbf{k}) = \varepsilon(\mathbf{k}) - \mu_0$ and $\varepsilon(\mathbf{k})$ is the dispersion law $\varepsilon(\mathbf{k}) = \sum_i T_{0i}e^{i\mathbf{k}\cdot\mathbf{R}_i}$.

In order to investigate the Hamiltonian in Eq. (1), we use the Keldysh nonequilibrium Green's function formalism. For the details of the formalism, we refer the reader to the original article[5] and the review by Rammer and Smith[22]. At time $t_0 = 0$, the system is prepared in thermal equilibrium at temperature $T_0$ with $E(t_0) = U(t_0) = 0$. Then one can study various profiles of turning on $U(t)$ and $E(t)$.

The matrix Green's function is expressed using creation/annihilation operators in the Heisenberg representation as

$$\underline{\underline{G}}_{\mathbf{k}\sigma}(t,t') = G^{\alpha\beta}_{\mathbf{k}\sigma}(t,t') = -i\langle T_C\, \hat{c}_{\mathbf{k}\sigma}(t_\alpha)\hat{c}^\dagger_{\mathbf{k}\sigma}(t'_\beta)\rangle_0 \tag{5}$$

where $T_C$ is the time-ordering operator along the Keldysh contour; indices $\alpha, \beta = \pm$, determine whether the corresponding time lies on the forward or return branch of the Keldysh contour; and $\langle ...\rangle_0$ denotes the thermal average with respect to the initial noninteracting thermal density matrix

$$\langle ...\rangle_0 = \frac{\mathrm{Tr}(\hat{\rho}_0 ...)}{\mathrm{Tr}(\hat{\rho}_0)}\ , \qquad \hat{\rho}_0 = e^{-\hat{H}(t_0)/T_0} \tag{6}$$

with $T_0$ being the temperature at $t_0$ (and the vector potential vanishes at $t_0$). Analytic formulas for the noninteracting Green's functions $\underline{\underline{G}}^0_{\mathbf{k}\sigma}(t,t')$ have been derived in Refs. 23 and 24. We would like to emphasize that those are exact solutions for the Hamiltonian in Eq. (4), which means that the electric field is taken into account *non-perturbatively*. So in the following by the term "noninteracting" we mean functions where the electric field is included, but the interaction between electrons is not.

The matrix Green's function in Eq. (5) obeys the Dyson equation

$$\underline{\underline{G}}_{\mathbf{k}\sigma} = \underline{\underline{G}}_{0,\mathbf{k}\sigma} + \underline{\underline{G}}_{0,\mathbf{k}\sigma} \otimes \underline{\underline{\Sigma}}_{\mathbf{k}\sigma} \otimes \underline{\underline{G}}_{\mathbf{k}\sigma} \tag{7}$$

where the symbol $\otimes$ denotes the time convolution and matrix multiplication

$$(\underline{\underline{A}} \otimes \underline{\underline{B}})^{\alpha\beta}(t,t') = \int_{t_0}^{+\infty} \sum_\gamma A^{\alpha\gamma}(t,t_1)B^{\gamma\beta}(t_1,t')dt_1. \tag{8}$$

For the Hubbard Hamiltonian in Eq. (4), the charge current density operator is

$$\hat{j}_{\alpha\sigma}(t) = \frac{e}{N\hbar}\sum_{\mathbf{k}} \frac{\partial}{\partial k_\alpha}\varepsilon[\mathbf{k}-\mathbf{A}(t)]\hat{c}^\dagger_{\mathbf{k}\sigma}\hat{c}_{\mathbf{k}\sigma} \tag{9}$$

where $N$ is the total number of lattice sites, and the current density can be found using the equal-time lesser Green's function[24] $G^< = G^{+-}$

$$j_{\alpha\sigma}(t) = -\frac{i}{N}\sum_{\mathbf{k}} G^<_{\mathbf{k}\sigma}(t,t)\frac{\partial}{\partial k_\alpha}\varepsilon[\mathbf{k}-\mathbf{A}(t)]. \tag{10}$$

The lesser Green's function $G^<_{\mathbf{k}\sigma}(t,t')$ also allows one to calculate the thermal average (per unit cell) of the double occupancy operator $\hat{D} = \sum_i \hat{n}_{i\sigma}\hat{n}_{i\bar{\sigma}}$

$$D(t) = \frac{i}{NU(t)}\sum_{\mathbf{k}} \lim_{t'\to t}\left\{-i\partial_t - \mu_0 + \varepsilon\big[\mathbf{k}-\mathbf{A}(t)\big]\right\}G^<_{\mathbf{k}\sigma}(t,t'), \tag{11}$$

and the total energy of the system per unit cell satisfies

$$E_{tot}(t) = \frac{i}{N}\sum_{\mathbf{k}} \lim_{t'\to t}\left\{-i\partial_t - \mu_0 - \varepsilon\big[\mathbf{k}-\mathbf{A}(t)\big]\right\}G^<_{\mathbf{k}\sigma}(t,t'). \tag{12}$$

For the sake of brevity we will omit the "per unit cell" wording and refer to these quantities as the total current, the double occupancy and the total energy for the remainder of the paper.

When the shift $U(t)n_{\bar{\sigma}}$ of the chemical potential is incorporated into the noninteracting Green's functions (*i. e.* perturbation theory is implemented in terms of the Hartree-Fock Green's functions), we have only a single diagram for the second-order contribution to the self-energy shown in Fig. 1.

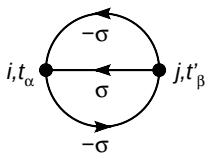


FIG. 1: Second-order contribution to the self-energy. The solid dot vertices correspond to the interaction $U$ and time changes along the horizontal direction. The solid lines represent either the Hartree-Fock (SOPT), or the dressed (self-consistent SOPT) Green's function, or the effective medium for the equivalent impurity problem (IPT).

When the lines correspond to the Hartree-Fock Green's functions, we obtain the second-order perturbation theory (SOPT). If we use the dressed Green's functions for the lines, we obtain the self-consistent SOPT. Thus for the self-consistent SOPT case the corresponding formula is

$$\Sigma^{\alpha\beta(2)}_{ij,\sigma}(t,t') = U(t)G^{\alpha\beta}_{ij,\sigma}(t,t')G^{\beta\alpha}_{ji,\bar{\sigma}}(t',t)G^{\alpha\beta}_{ij,\bar{\sigma}}(t,t')U(t'). \tag{13}$$

We use the limit of infinite dimensions on the hypercubic lattice with nearest neighbor ($nn$) hopping, introduced in Ref. 25, which simplifies calculations tremendously. In this limit, the hopping is scaled as $T_{nn} = \frac{t^*}{2\sqrt{d}}$ ($d$ is the space dimension and $t^*$ is the hopping energy unit), the density of states becomes a Gaussian

$$\rho_0(\varepsilon) = \frac{1}{t^*\sqrt{\pi}} \exp\left(-\frac{\varepsilon^2}{t^{*2}}\right) \tag{14}$$

and the self-energy becomes local[26]

$$\underline{\underline{\Sigma}}_{ij,\sigma} = \underline{\underline{\Sigma}}_{ii,\sigma}\delta_{ij} \ , \quad \underline{\underline{\Sigma}}_{\mathbf{k}\sigma} = \underline{\underline{\Sigma}}_{ii,\sigma}. \tag{15}$$

The spatially uniform electric field $\mathbf{E}(t)$ is created by the vector potential, aligned along the main diagonal of a hypercube,

$$\mathbf{A}(t) = A(t)(1,1,...) \ . \tag{16}$$

For this choice of the vector potential, current density components $j_{\alpha\sigma}$ turn out to be identical for each axis, and due to the scaling of the hopping, they vanish as $\sim 1/\sqrt{d}$, but the current density along the main diagonal $j_\sigma$ remains finite. In numerical calculations we always plot this nonvanishing component.

The computational scheme is realized as follows. We calculate the Hartree-Fock Green's functions $\underline{\underline{G}}_{0,\mathbf{k}\sigma}$ using analytic relations. Summation over $\mathbf{k}$ gives us the local Hartree-Fock Green's functions so that we can calculate the second-order self-energies from Eqs. (13) and (15). Then we solve the Dyson equation in Eq. (7) numerically and find the dressed Green's function $\underline{\underline{G}}_{\mathbf{k}\sigma}$. Equation (7) is a linear Volterra matrix equation of the second kind and allows a very efficient numerical integration[27]. The solution obtained this way will be the SOPT solution. If we want to obtain the self-consistent SOPT solution, we use the SOPT Green's function $\underline{\underline{G}}_{\mathbf{k}\sigma}$ as a first approximation. Then summing over $\mathbf{k}$ we obtain a local dressed Green's function $\underline{\underline{G}}_{ii,\sigma}$, use it to calculate new values for the self-energies in Eqs. (13) and (15) and repeat all the previous steps until the dressed Green's functions converge. Then the lesser Green's function $G^<_{\mathbf{k}\sigma}(t,t')$ is used to find the charge current, the total energy and the double occupancy according to Eqs. (10–12).

This approach can also be generalized to IPT. In that case, one needs to write additional equations for the impurity model and the self-energy diagram in Fig. 1 is applied to the impurity Hamiltonian instead of the lattice one. We will not discuss the details of the IPT scheme here and instead refer the reader to articles by Amaricci, *et al.*[28] and Eckstein and Werner[29]. Our approach is different from those only in the absence of imaginary time piece of the contour, which is always valid if one starts from the noninteracting thermal state.

## III. LONG TIME APPLICABILITY AND SERIES RESUMMATION

An issue for using perturbation theory is its applicability for different parameter regimes. In the nonequilibrium formalism, a perturbation expansion is expressed in powers of

$$\int_{t_0}^{t_{max}} \hat{H}_i(t)dt \ , \tag{17}$$

where $\hat{H}_i(t)$ is the interaction part of the Hamiltonian in Eq. (1), written in Heisenberg representation, and $t_{max}$ should be larger than any of the external times (*i.e.*, times over which there is no integration). For a time independent $\hat{H}_i(t)$ the integral in Eq. (17) grows linearly with $t_{max}$, so that the terms the order of $k$ in the interaction grow as $t^k_{max}$, which can lead to a divergence of the results if a resummation of the diagrams is not done properly. This can be best seen if we consider the Hartree-Fock diagram for the self-energy, which is shown in Fig. 2. For time-independent $U$, this diagram gives the self-energy matrix

$$\underline{\underline{\Sigma}}^{HF}_{ii,\sigma}(t) = -iUG^<_{0,ii,\bar{\sigma}}(t)\,\underline{\underline{1}} = Un_{0,\bar{\sigma}}\cdot\,\underline{\underline{1}} \ , \tag{18}$$

where $\underline{\underline{1}}$ is the unit 2 by 2 matrix. Instead of a numerical solution of the Dyson equation in Eq. (7), we can write

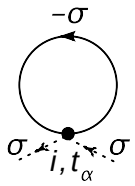


FIG. 2: Hartree-Fock self-energy diagram for the Hubbard model

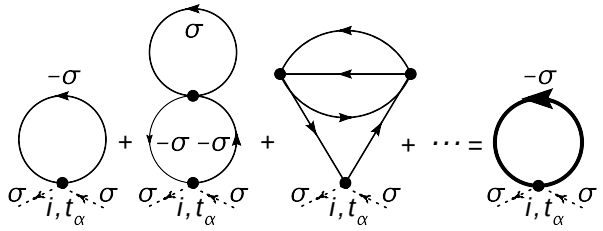


FIG. 3: Single time self-energy diagrams for the Hubbard model

it as an infinite series

$$\underline{\underline{G}}_{\mathbf{k}\sigma} = \underline{\underline{G}}_{0,\mathbf{k}\sigma} + \underline{\underline{G}}_{0,\mathbf{k}\sigma} \otimes \underline{\underline{\Sigma}}_{\mathbf{k}\sigma} \otimes \underline{\underline{G}}_{0,\mathbf{k}\sigma} + \\ + \underline{\underline{G}}_{0,\mathbf{k}\sigma} \otimes \underline{\underline{\Sigma}}_{\mathbf{k}\sigma} \otimes \underline{\underline{G}}_{0,\mathbf{k}\sigma} \otimes \underline{\underline{\Sigma}}_{\mathbf{k}\sigma} \otimes \underline{\underline{G}}_{0,\mathbf{k}\sigma} + ... \tag{19}$$

and try to calculate the dressed Green's function using the explicit expression in Eq. (19). For the self-energy in Eq. (18), the inner integrations can be done analytically, leading to the result

$$\underline{\underline{G}}_{\mathbf{k}\sigma}(t,t') = \Big(1 + iUn_{0,\bar{\sigma}}(t'-t) + \\ + \tfrac{1}{2}\big(iUn_{0,\bar{\sigma}}(t'-t)\big)^2 + ...\Big)\, \underline{\underline{G}}_{0,\mathbf{k}\sigma}(t,t') \tag{20}$$

which sums up to

$$\underline{\underline{G}}_{\mathbf{k}\sigma}(t,t') = \exp\Big(-iUn_{0,\bar{\sigma}}(t-t')\Big)\, \underline{\underline{G}}_{0,\mathbf{k}\sigma}(t,t') \tag{21}$$

From Eq. (20), we see that the truncation of the Dyson equation after the $k$-th power in $U$ leads to results which diverge as $U^k(t-t')^k$ and only an exact summation of the infinite series in Eq. (19), or, which is the same, a numerical solution of the Dyson equation in Eq. (7), correctly reproduces the oscillating exponent in Eq. (21).

For a paramagnetic solution, we can generalize Eq. (21) and claim that by using the Dyson equation, the single time part of the self-energy can be accounted for exactly with the formula

$$G^R_{\mathbf{k}\sigma}(t,t') = \exp\left(-i\int_{t'}^{t}\Sigma_{\bar{\sigma}}(t_1)dt_1\right) G^R_{0,\mathbf{k}\sigma}(t,t')$$

In the case of the Hamiltonian in Eq. (1), the sequence of diagrams producing the single time part of the self-energy is shown in Fig. 3 and sums up to the dressed Green's function so that the self-energy is

$$\underline{\underline{\Sigma}}^{HF}_{ii,\sigma}(t) = -iU(t)G^{<}_{ii,\bar{\sigma}}(t)\,\underline{\underline{1}} = U(t)n_{\bar{\sigma}}\cdot\,\underline{\underline{1}}\,, \tag{22}$$

which means that we can analytically calculate the Hartree-Fock Green's function and therefore perform subsequent perturbation theory in relative to this function.

There are no inner integrations in the second-order self-energy diagram in Fig. 1, however there are inner integrations in higher-order diagrams, so one can still ask whether these can lead to terms that are divergent as $t \to \infty$. In fact they do diverge[33], so in nonequilibrium calculations one has to regularize these terms by using a series resummation procedure, though it is not always clear how this can be done.

One may think that the divergence of the perturbation expansion terms at large times is unique to the nonequilibrium formalism, and, for example, in Matsubara formalism, such an issue can never occur because the expansion is performed in powers of

$$\int_0^{\beta}\hat{H}_i(\tau)d\tau$$

where the integration interval is fixed, therefore it may seem that the summation of an infinite series in not necessary, since taking enough expansion terms we can improve our expansion as far as it is desired. But this is not exactly so. Writing the Dyson equation as an infinite series

$$G_{\mathbf{k}\sigma}(i\omega_n) = G^0_{\mathbf{k}\sigma}(i\omega_n) + G^0_{\mathbf{k}\sigma}(i\omega_n)Un_{\bar{\sigma}}G^0_{\mathbf{k}\sigma}(i\omega_n) + \\ + G^0_{\mathbf{k}\sigma}(i\omega_n)Un_{\bar{\sigma}}G^0_{\mathbf{k}\sigma}(i\omega_n)Un_{\bar{\sigma}}G^0_{\mathbf{k}\sigma}(i\omega_n) + ... \tag{23}$$

we can find the resulting density of states (DOS)

$$\rho(\omega) = \Big(1 + 2Un_{\bar{\sigma}}(\omega+\mu) + 2U^2n^2_{\bar{\sigma}}(\omega+\mu)^2 + ...\Big)\rho_0(\omega+\mu) \tag{24}$$

where $\rho_0$ is the noninteracting DOS in Eq. (14). The prefactors to the exponent diverge at large frequencies and although the exponent prevents the divergence, it is obviously unphysical, since Eq. (24) gives a negative DOS as $\omega \to \infty$. Only the summation of all terms in Eq. (24) produces the correct result

$$\rho(\omega) = \rho_0(\omega + \mu - Un_{\bar{\sigma}}) \tag{25}$$

In this sense the equilibrium result in Eq. (24) is a direct analog of the nonequilibrium result in Eq. (20), because any truncation of the perturbation series expansion leads to unphysical results. Thus the Keldysh formalism and the Matsubara formalism have similar convergence issues, but in the Matsubara formalism these issues are hidden by the finiteness of the imaginary time interval

and by the simplicity of the Dyson equation, which reduces to a simple algebraic equation, as opposed to the integral equation in Eq. (7).

Up to now we have considered the simple case of the Hartree-Fock self-energy, which had no inner integrals, and therefore the infinite series summation was needed only for the Green's function calculation. But higher order self-energy contributions have internal vertices, over which the integration must be performed. In this case, regularization of the large time divergences leads to Dyson-like equations for the calculation of the self-energy too.

One may question the validity of the perturbation expansions at large times, since regularization of the divergent terms does not guarantee the precision of the results. We think that this question should be answered individually in each case, taking into account how good the observables, which should be conserved, are conserved, how physical the results are and so on. But if we want to advocate the nonequilibrium perturbation expansion, we can say that higher-order self-energy expansions in the Matsubara formalism will suffer from the same problems at large frequencies as higher-order self-energy expansions in Keldysh formalism at large times, if resummation of diagrams is not done properly.

## IV. NUMERICAL RESULTS

We present the results of SOPT, self-consistent SOPT and IPT calculations of the nonequilibrium current, double occupancy, total energy and Green's functions as functions of time for a half-filled metal. In equilibrium, perturbative approaches provide reliable results when $U$ is far from metal-insulator transition, which happens at[30] $U_c(T=0) \approx 4.1$. The initial state of the system is noninteracting ($U=0$) and is in thermal equilibrium at an initial temperature $T_0$. In all calculations presented in this article, unless noted otherwise, the electric field $\mathbf{E}$ and Hubbard $U$ are turned on simultaneously at $t=0$, thus one should remember that temperatures $T_0$ given for each plot characterize only the initial total energy of the system, since an additional energy of $\frac{1}{4}U$ is instantaneously pumped into the system due to the sudden change of $U$ at $t=0$ and then subsequent Joule heating can further change the energy when a current flows. On the plots, the energy and temperature are measured in units of hopping energy $t^*$, time – in units of $\hbar/t^*$, the electric field – in units of $t^*/(ea)$, where $a$ is the lattice constant, and the current density – in units of $et^*/(\hbar a^{d-1})$.

### A. No electric field

In order to check our numerical scheme and compare different methods, we consider first the case without the electric field. From the equilibrium calculations, we know that all the three methods work well for small $U$-regimes, but the SCSOPT is unable to show the formation of the side bands as $U$ is increased (see Fig. 4). The SOPT is able to capture the side bands formation, but becomes less reliable compared to the IPT for large $U$'s. This

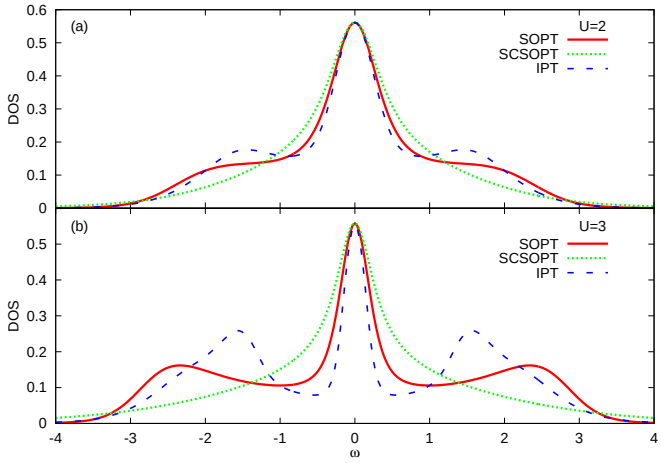


FIG. 4: (color online) The equilibrium density of states (DOS) versus frequency $\omega$, calculated using SOPT (solid), SCSOPT (dotted) and IPT (dashed) at $T=0.01$ for (a) $U=2$ and (b) $U=3$.

equilibrium experience agrees well with the nonequilibrium calculations, shown in Fig. 5, panels (a) and (c), when the interaction $U(t)$ is turned on linearly from 0 to $U$ during the time interval $[0,19]$. We see that the final total energy in SCSOPT differs also from that of the SOPT and IPT calculations, which are very close to each other and the difference grows as $U$ is increased, because the density of states in SCSOPT deviates more and more from the SOPT and IPT density of states, as seen in Fig. (4).

The situation changes for the case of an interaction quench[15], shown in panels (b) and (d), when $U(t) = U\theta(t)$. Since the Hamiltonian in Eq. (1) becomes time independent, the total energy should be conserved. However, we see that the SOPT always loses energy. For example, for the case $U=2$, shown in panel (c), the additional energy, pushed into the system, should lead to the final temperature $T \approx 0.47$ after the system reaches thermal equilibrium. Instead, the final energy corresponds to a temperature of $\sim 0.057$. This behavior of the SOPT was observed for the range of values $U \leq 3$ and also for an initial temperature $T_0 = 0.1$ - the scheme cools down to the initial temperature, "forgetting" about the additional energy pumped into it by the sudden change of $U$. This is a problem that can occur for approximations that are not conserving.

The results produced by SCSOPT and IPT look more reliable for $U=2$ (panel (b)). The SCSOPT conserves the total energy much better than the IPT does. Due to the difference in energy ranges between panels (a) and (b) one may think that the situation in nonequilibrium is worse for the IPT, but it is not the case and the difference

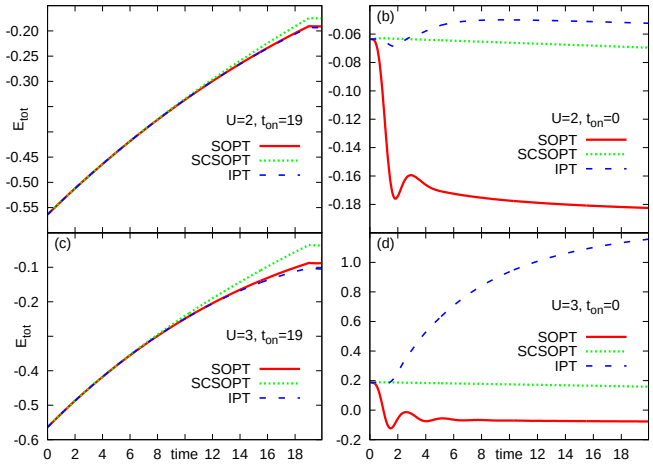


FIG. 5: (color online) Nonequilibrium total energy for (a) $U = 2$, $t_{on} = 19$, (b) $U = 2$, $t_{on} = 0$, (c) $U = 3$, $t_{on} = 19$, (d) $U = 3$, $t_{on} = 0$, versus time calculated using SOPT (solid), SCSOPT (dotted), and IPT (dashed) for $T_0 = 0.01$.

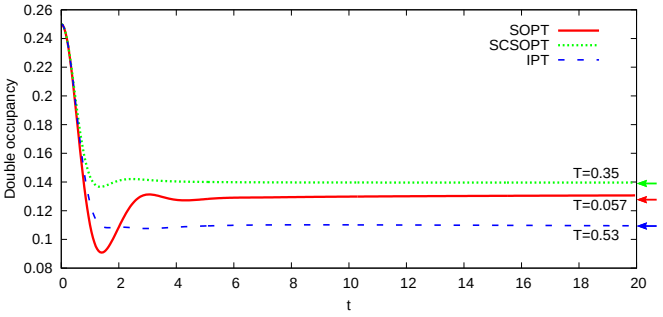


FIG. 6: (color online) Double occupancy for the interaction quench with $U = 2$ in (red solid) SOPT, (green dotted) SCSOPT, (blue dashed) IPT.

between final total energy in the SCSOPT and IPT is almost the same for panels (a) and (b). For the case $U = 3$ the SOPT results become worse, the IPT fails completely (the total energy starts to grow around $t \sim 2$) and only the SCSOPT calculations produce reasonable results.

We can conclude that for processes where the interaction changes slowly and the system stays close to thermal equilibrium, the relation between the SOPT, IPT and SCSOPT remains the same as in equilibrium: the SOPT and IPT produce similar and most trustworthy results, because they are more reliable in calculating the static DOS, while the precision of the SCSOPT calculations becomes worse as $U$ becomes larger. But when the system parameters change fast, the SOPT is unable to capture the thermodynamics of the process. This means it is still able to calculate the static DOS properly, but it is not able to calculate the electron distribution changes and forces the system to restore the initial temperature. This is the so called memory of the initial state[14]. At the same time, the IPT and SCSOPT remain suitable methods for calculating the fast electron distribution evolution, although the IPT fails at some critical value of $U$, unlike the equilibrium situation, where the IPT is able to describe the insulating (*i.e.* large $U$) regime as well (when at half-filling).

In order to investigate the issue of the thermalization of the system, we follow the procedure of Eckstein *et al.*[15] and plot the double occupancy for the interaction quench $U(t) = U\theta(t)$. Fig. 6 shows the double occupancy for $U = 2$. For each curve we take $E_{tot}(t = 19.9)$ and calculate the equilibruim double occupancy corresponding to this value. This equilibrium double occupancy is shown by the arrows. For each nonequilibrium method, the equivalent equilibrium method is used, *i.e.*, for the nonequilibrium SOPT the corresponding double occupancy is calculated using the equilibrium SOPT and so on. The plot shows that for all methods the system converges to the corresponding equilibrium value. Calculations for the range of $U \leq 2$ show that for the SCSOPT and IPT the difference between the final nonequilibrium double occupancy and the corresponding equilibrium one is less then 0.3%, and for the SOPT it is around 0.3% for $U = 0.25$ and around 2% for $U = 2$.

### B. Constant electric field

In Fig. 7, we plot the current density, total energy and double occupancy for $T_0 = 0.1$ (black, SOPT calculation), $T_0 = 1$ (bold red, SOPT calculation) and $T_0 = 0.1$ (black dotted, IPT calculation). The system is a metal ($U = 0.25$) placed in a diagonal electric field with the same components $E_\alpha(t) = E\theta(t)$ along each axis and $E = 1$.

The SOPT current density (upper panel, solid lines) is a sine function with period $2\pi\hbar/(eaE)$ (or $2\pi/E$ in the units used for plotting), modulated by a time-dependent amplitude. The main oscillation period, as well as the physical mechanism of the origin of the oscillating current, is the same as for the Bloch oscillations in the noninteracting case[24]. The modulation produces beats, which become smaller with time, however do not vanish up to the largest times we have studied, which is $t_{max} = 400$; the period of the beats decreases as the initial temperature increases, which can be seen most easily on the double occupancy panel. Higher initial temperatures also reduce the amplitude of the current density oscillations. The IPT curve ($T_0 = 0.1$, dotted lines) shows a very different behavior. Up to $t \approx 30$ the current coincides with the SOPT result, but then the oscillation amplitude continues to decline, while the SOPT amplitude shows beats.

The current density plots in Fig. 7 show a dependence of the system behavior on its initial temperature, despite the fact that additional energy is pumped into the system by the electric field. The total energy oscillations (middle panel) have a phase shift of $\pi/2$ with respect

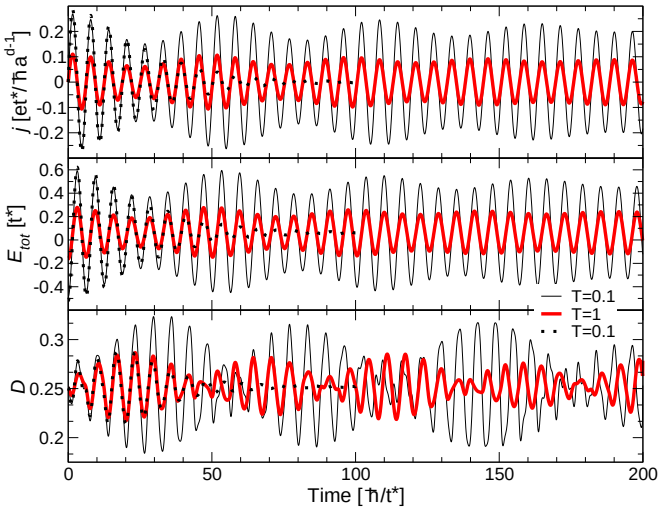


FIG. 7: (color online) Nonequilibrium (a) current density, (b) total energy and (c) double occupancy versus time for different values of $T_0$ with $E = 1$, $U = 0.25$. Solid black lines correspond the SOPT with $T_0 = 0.1$, solid bold red lines correspond to the SOPT with $T_0 = 1$, and dotted lines to the IPT calculation with $T_0 = 0.1$.

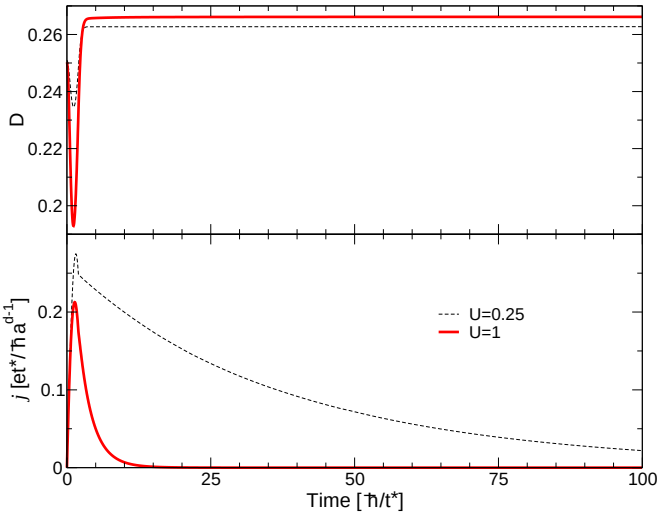


FIG. 8: (color online) Nonequilibrium (a) double occupancy and (b) current density versus time in the self-consistent SOPT for different values of $U$ for a pulsed field with $E = 1$, $T_0 = 0.1$, $t_f = 2$.

to the current density, in agreement with the relationship $dE_{tot}(t)/dt = \mathbf{E} \cdot \mathbf{j}$. This relationship reflects the fact, that the system energy increases, whenever there is a current $\mathbf{j}$ in the direction of the electric field $\mathbf{E}$, and decreases, when the direction of the current is opposite. The double occupancy (lower panel) is oscillating close to the noninteracting value of 0.25. The main oscillation period is the same as for the current density, but a slow temperature-dependent modulation is now present in both the amplitude and the phase of the oscillations. Note that for the half-filled model in thermal equilibrium, the repulsive $U$ (*i. e.* $U > 0$) always leads to a double occupancy tht satisfies $D < 0.25$, while values $D > 0.25$ are possible only for attractive $U$. Since we consider only a repulsive interaction here, the transient times where the double occupancy satisfies $D > 0.25$ should be viewed as a signature of nonequilibrium effects.

On the other hand, calculations within the IPT (Fig. 7, dotted curves) show that in the long time limit the system always approaches the thermal equilibrium state with $T = \infty$: the current vanishes, the total energy and the double occupancy approach $E_{tot} = 0$ and $D = 0.25$ respectively, and the single particle distribution function (not plotted here) shows that all available states are occupied with the same probability[31]. This scenario of heating the system to an infinite temperature is discussed in Refs. 18 and 29. Of course, such situation never occurs in a real system (which is attached to some form of a heat bath), since the heat is always removed somehow[28], but if a mechanism for heat removal is weak, the temperature can rise significantly.

The self-consistent SOPT calculations (not shown in Fig. 7) agree well with the IPT results both qualitatively and quantitatively: current, total energy and the double occupancy coincide within about 5% up to $t \approx 50$, but for larger times IPT results show a faster decay. Thus we can conclude that in presence of the electric field, the SOPT is reliable for small time scales only, unlike the equilibrium case, where the precision of the SOPT depends solely on the value of the Coulomb interaction $U$.

### C. Pulsed electric field

In this subsection, we examine the case when the electric field is acting only within a finite time interval $t \in [0, t_f]$, $E_\alpha(t) = E\theta(t)\theta(t_f - t)$. For all the cases studied below, we have verified that the IPT and the self-consistent SOPT results are visually indistinguishable, so we choose the latter, since it is less computationally demanding, therefore we can do calculations using a finer energy grid for higher accuracy.

In Fig. 8, we plot the double occupancy and current density for $U = 0.25$ (black) and $U = 1$ (bold red) for $E = 1$, $T_0 = 0.1$, and $t_f = 2$ calculated within self-consistent SOPT. Once the electric field is turned off, the double occupancy relaxes to a constant value after a characteristic time $\approx 1$, which is consistent with an estimate $\tau_e \approx \frac{\hbar}{t^*}$ of the time between electron-electron collisions in the half-filled tight binding model. The current decay can be fit by $j(t) \approx j(t_f)\exp(-U^2(t - t_f)/2)$, thus the characteristic time for current decay turns out to be inversely proportional to $U^2$ in accordance with Boltzmann equation results[29].

This vanishing of the current after the electric field is turned off is due to the noncommutativity of the Hamil-

tonian in Eq. (1) with the charge current operator in Eq. (9). Thus the simultaneous presence of both the lattice and the Coulomb interaction provides another mechanism for breaking quasi-momentum conservation, in addition to introducing a thermal bath, as suggested in Ref. 28.

It is interesting to note that for small $U$ and short electric field pulses the SOPT produces results which are almost identical to those of the self-consistent SOPT. Thus the SOPT is accurate for short times, and only fails when the electric field is present for longer times.

The current and the double occupancy behavior suggest that at $t = 100$ for both $U = 0.25$ and $U = 1$, the system reaches some stationary state. Notice that the final values of the double occupancy are larger than 0.25 and increase with the increase of $U$, which is impossible in thermal equilibrium for repulsive $U$.

In order to investigate the origin of this phenomenon, we plot the single-particle distribution function $n(\varepsilon, \bar{\varepsilon}; t) = -iG^{<}_{\varepsilon,\bar{\varepsilon}}(t, t)$. As discussed in Ref. 32, when the **E**-field is aligned along the main diagonal of the hypercube, the **k**-dependence of the Green's functions can be reduced to the dependence on two "energies" $\varepsilon_{\mathbf{k}}$ and $\bar{\varepsilon}_{\mathbf{k}}$, compared to the case without an electric field, where we have the dependence of all functions only on $\varepsilon_{\mathbf{k}}$. In Fig. 9, we plot $n(\varepsilon, \bar{\varepsilon}; t = 100)$ for $E = 1$, $U = 0.25$, $T_0 = 0.1$, and $t_f = 1.625$. If the system has reached a thermal equilibrium, the resulting distribution must be independent of $\bar{\varepsilon}$, while along the $\varepsilon$-axis we would have a thermal distribution, corresponding to some temperature $T$ (and perhaps broadened due to the interactions). Instead, we have a strong $\bar{\varepsilon}$-dependence and the $\varepsilon$-dependence is far from thermal, especially for $\bar{\varepsilon} \approx 0$, where $n(\varepsilon, \bar{\varepsilon})$ has a jump at the Fermi energy $\varepsilon = 0$, but does not vanish for large $\varepsilon$'s. Therefore at large times the system is stuck in a quasistationary nonequilibrium state. It is exactly this nonequilibrium state, which is responsible for values of the double occupancies which are incompatible with a thermal state.

In Fig. 10, we plot the imaginary part of the Keldysh Green's function $\mathrm{Im}G^{K}_{\varepsilon\bar{\varepsilon}}(t_1, t_2)$ as a function of times $t_1, t_2$ for a pulsed field with $E = 1$, $U = 0.25$, $T_0 = 0.1$, $t_f = 3$, and with fixed $\varepsilon = -2.625$ and $\bar{\varepsilon} = 1.125$. We see that whenever $t_1 \lessapprox 5$ or $t_2 \lessapprox 5$ the Keldysh function depends on both the average, $t_a = (t_1 + t_2)/2$, and the relative, $t_r = t_1 - t_2$, times. But when $t_1 \gtrapprox 5$ and $t_2 \gtrapprox 5$ this function becomes independent of $t_a$ (*i. e.* the height of the surface in Fig. 10 does not change as we move along lines $t_2 = t_1 + \text{const}$.). The same holds for the real part of the Keldysh Green's function, as well as for the real and imaginary parts of the retarded Green's function for all values $(\varepsilon, \bar{\varepsilon})$. Thus we see that the nonequilibrium states of the system, created by a pulsed $E$-field are so called steady states, *i. e.* states independent of the average time.

We can summarize our findings by saying that using an electric field pulse we force a system into a long-lived nonequilibrium steady state. It was argued by Moeckel and Kehrein[16] that for small values of the Coulomb interaction, the full thermalization happens on timescales of the order of $\tau_{therm} \sim \rho_0^{-3}(0)U^{-4}$, so by long-lived we mean that this nonequilibrium steady state does not thermalize even on this time scale.

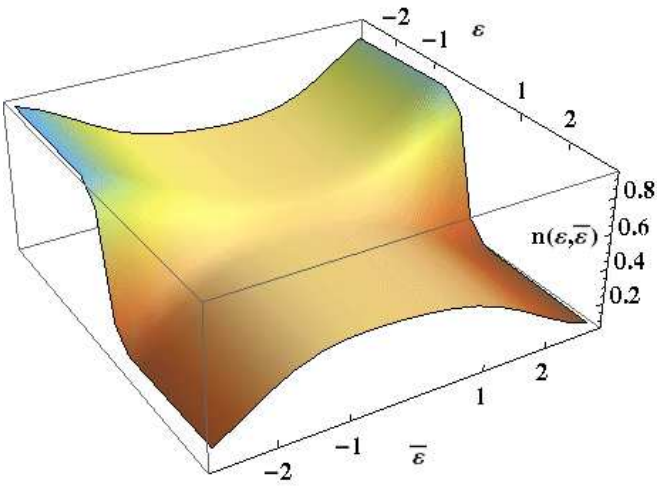


FIG. 9: (color online) Particle distribution function in the self-consistent SOPT at $t = 100$ for a pulsed field with $E = 1$, $U = 0.25$, $T_0 = 0.1$, $t_f = 1.625$.

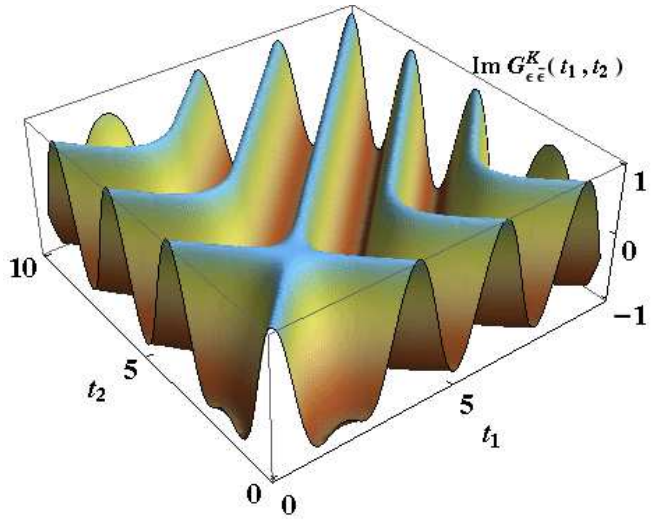


FIG. 10: (color online) $\mathrm{Im}G^{K}_{\varepsilon\bar{\varepsilon}}(t_1, t_2)$ as a function of two times $t_1, t_2$ for the pulsed field with $E = 1$, $U = 0.25$, $T_0 = 0.1$, $t_f = 3$, and with fixed $\varepsilon = -2.625$ and $\bar{\varepsilon} = 1.125$.

In order to investigate, how the double occupancy of the resulting nonequilibrium steady state depends on the length of the E-field pulse $t_f$, we plot the double occupancy measured at $t = 50\hbar/t^*$ versus $t_f$ in Fig. 11. When $t_f = 0$, the double occupancy $D(t = 50)$ corresponds to some equilibrium thermal state and is always less than 0.25. Depending on the length of the pulse, we can achieve $D \approx 0.27$ for $T_0 = 0.1$ and $U = 0.25$. As we can see from Fig. 8 even higher double occupancies

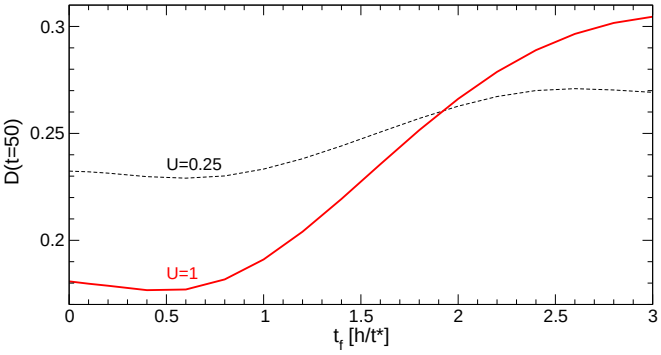


FIG. 11: (color online) Double occupancy versus the length of the E-pulse $t_f$ in the self-consistent SOPT measured at $t = 50$ for $T_0 = 0.1$, $E = 1$, $U = 0.26$ (dashed black) and $U = 1$ (bold red).

can be achieved for $U = 1$. The double occupancies for both values of $U$ achieve maximums when $\int_0^{t_f} E_\alpha(t)dt$ is roughly $\pi$ in agreement with the prediction in Ref. 20, however we believe that the final distribution of the electrons in Fig. 9 cannot be described by the effect of a negative temperature only and is, in fact, a nonequilibrium distribution.

## V. CONCLUSIONS

We have shown how various properties of a nonequilibrium state of the Hubbard model in a spatially uniform electric field can be calculated perturbatively in the Coulomb interaction $U$. Such calculations are computationally inexpensive and allow us to access times much longer than other existing methods, so that even a transition of the system to the steady state can be studied. We have shown that when the interacting system without the external bath in the metallic state is placed into a DC electric field the Bloch oscillations of the current are suppressed by the heating of the system to infinite temperature.

We have also shown that a short electric field pulse can create a steady (*i. e.* average time independent) nonthermal state, which can exist for times longer than the available theoretical estimates of lifetimes for nonthermal states.

One might think that the presence of this steady state is just an artifact of the truncation of the perturbation series. Indeed, at strong coupling this can occur if the interaction strength is much larger than the hopping, because relaxation processes require multiparticle effects. But here we have a weak $U$ and the perturbation theory is a self-consistent one, so it includes many high-order diagrams. Hence, it is unlikely that these effects arise solely from the truncation of the perturbation theory. For large $U$, there is evidence that steady states can occur even for continuously driven systems[19], but the scenario for thermalization is more complex than what is seen here at weak coupling.

### Acknowledgments

We would like to thank V. Turkowski, O. Peil, A. Shvaika, M. Eckstein, P. Arseev and E. Altman for fruitful discussions. A.J. and A.L. acknowledge support from DFG SFB-925 and CUI-cluster of excellence. Initial stage of this work was done at Universität Augsburg and many discussions with Prof. D. Vollhardt, as well as support from DFG Sonderforschungsbereich 484, are acknowledged. J.K.F. acknowledges the National Science Foundation under grant number DMR-1006605 and the McDevitt bequest at Georgetown University.

* Electronic address: Alexander.Joura@physnet.uni-hamburg.de
† Electronic address: alichten@physnet.uni-hamburg.de

[1] A. L. Cavalieri, N. Müller, Th. Uphues, V. S. Yakovlev, A. Baltuška, B. Horvath, B. Schmidt, L. Blümel, R. Holzwarth, S. Hendel, M. Drescher, U. Kleineberg, P. M. Echenique, R. Kienberger, F. Krausz, and U. Heinzmann, Nature **449**, 1029 (2007); R. I. Tobey, D. Prabhakaran, A. T. Boothroyd, and A. Cavalleri, Phys. Rev. Lett. **101**, 197404 (2008).
[2] O. Morsch, J. H. Müller, M. Cristiani, D. Ciampini, and E. Arimondo, Phys. Rev. Lett. **87**, 140402 (2001).
[3] S. Mandt, A. Rapp, and A. Rosch, Phys. Rev. Lett. **106**, 250602 (2011).
[4] L. P. Kadanoff and G. Baym, *Quantum Statistical Mechanics* (W. A. Banjamin, Inc., New York, 1962)
[5] L. V. Keldysh, Zh. Eksp. Teor. Fiz. **47**, 1515 (1964) [Sov. Phys. JETP **20**, 1018 (1965)].
[6] P. Schmidt and H. Monien, cond-mat/0202046; P. Schmidt, Diplom thesis, University of Bonn 1999.
[7] J. K. Freericks, V. M. Turkowski, and V. Zlatić, Phys. Rev. Lett. **97**, 266408 (2006).
[8] A. Georges, G. Kotliar, W. Krauth, and M.J. Rozenberg, Rev. Mod. Phys. **68**, 13 (1996).
[9] J. K. Freericks, Phys. Rev. B **77**, 075109 (2008)
[10] P. Werner, T. Oka, and A. J. Millis, Phys. Rev. B **79**, 035320 (2009)
[11] N. Tsuji, T. Oka, P. Werner, and H. Aoki, Phys. Rev. Lett. **106**, 236401 (2011)
[12] M. Rigol, V. Dunjko, and M. Olshanii, Nature **452**, 854 (2008).
[13] M. Cramer, C. M. Dawson, J. Eisert, and T. J. Osborne, Phys. Rev. Lett. **100**, 030602 (2008)
[14] M. Eckstein and M. Kollar, Phys. Rev. Lett. **100**, 120404 (2008).
[15] M. Eckstein, M. Kollar, and P. Werner, Phys. Rev. Lett. **103**, 056403 (2009).
[16] M. Moeckel and S. Kehrein, Phys. Rev. Lett. **100**, 175702

(2008).
[17] S. A. Hamerla and G. S. Uhrig, Phys. Rev. B **89**, 104301 (2014).
[18] M. Mierzejewski, L. Vidmar, J. Bonca, and P. Prelovsek, Phys. Rev. Lett. **106**, 196401 (2011).
[19] H. Fotso, K. Mikelsons, J. K. Freericks, *preprint* arXiv:1310.8354 (2013).
[20] N. Tsuji, T. Oka, H. Aoki, and P. Werner, Phys. Rev. B **85**, 155124 (2012).
[21] R. Peierls, Z. Phys. **80**, 763 (1933).
[22] J. Rammer and H. Smith, Rev. Mod. Phys. **58**, 323 (1986).
[23] A. P. Jauho and J. W. Wilkins, Phys. Rev. B **29**, 1919 (1984).
[24] V. Turkowski and J. K. Freericks, Phys. Rev. B **71**, 085104 (2005).
[25] W. Metzner and D. Vollhardt, Phys. Rev. Lett. **62**, 324 (1989).
[26] E. Müller-Hartmann, Z. Phys. B **74**, 507 (1989).
[27] M. Eckstein, M. Kollar and P. Werner, Phys. Rev. B **81**, 115131 (2010)
[28] A. Amaricci, C. Weber, M. Capone and G. Kotliar, Phys. Rev. B **86**, 085110 (2012).
[29] M. Eckstein and P. Werner, Phys. Rev. Lett. **107**, 186406 (2011).
[30] R. Bulla, Phys. Rev. Lett. **83**, 136 (1999)
[31] A. V. Joura, A. L. Lichtenstein, *unpublished*.
[32] V. Turkowski and J. K. Freericks, Phys. Rev. B **71**, 085104 (2005).
[33] A. V. Joura, A. L. Lichtenstein, *unpublished*.